

VHE Spectral Properties of Mrk 501 with the CAT telescope

J.P. Tavernet¹ for the CAT Collaboration

¹*L.P.N.H.E. Paris 6/7 - 4, Place Jussieu - 75252 Paris Cedex 05 - France*

Abstract

We report here observations of the active galactic nucleus Mrk 501, at energies above 250 GeV carried out with the CAT atmospheric imaging telescope from March 1997 to Autumn 1998. This source was in a high state of activity at several different wavelengths in 1997, and the observed flux at TeV energies has been seen to change by a factor of ~ 20 from 1995 and 1996 fluxes. CAT observations also indicate a curved spectrum at TeV energies, and a correlation between the gamma-ray intensity and the spectral hardness. The temporal variability and the TeV spectral properties are examined.

1 Introduction:

The active galactic nucleus (AGN) Mrk 501 is one of the closest ($z=0.034$) BL Lacertæ objects. It was discovered at TeV energies by the Whipple Observatory (Quinn et al., 1996), and confirmed by HEGRA (Bradbury et al., 1997) and the CAT collaboration (Punch et al., 1997).

From March to October 1997, VHE observations of Mrk 501 revealed extreme variability, with a measured flux up to 8 times the Crab Nebula flux. Several independent Čerenkov telescopes have confirmed this dramatic activity (Protheroe et al., 1998). Based on observations carried out in 1997, we present a detailed study of spectral properties. Thanks to the large variability of the source during this period, the spectral hardness was studied as a function of the intensity of the source and spectra were derived for different intensity levels.

Mrk 501 has been regularly observed by the CAT telescope since March 1997 and the resulting light curve is presented.

2 CAT Čerenkov Imaging Telescope and data analysis

Located on the Thémis solar plant in southern France (2°E , 42°N , 1650 m a.s.l.), the CAT (Čerenkov Array at Thémis) imaging telescope has been described in detail in Barrau et al. (1998). It achieves a low threshold (~ 250 GeV) despite its small reflector area (17.7 m²) by taking full advantage of the rapidity of the Čerenkov pulse with a near-isochronous mirror, fast phototubes, fast trigger and readout electronics. Moreover, its very high definition camera (546 pixels with an angular size of 0.12°) allows an accurate analysis of the longitudinal and lateral light profile of the shower image, as discussed in Le Bohec et al. (1998), giving a good separation of gamma-ray showers from hadronic ones by means of a χ^2 -like variable and of the pointing angle α .

Cuts used in the standard CAT analysis are the following: $P(\chi^2) > 0.35$, $\alpha \leq 6^\circ$, Q_{tot} (the total charge in the image) $\geq 30 \gamma e$; an additional cut requiring at least $3 \gamma e$ in the fourth-brightest pixel ensures uniform trigger conditions. These cuts yield a background rejection factor of about 200, with a γ -ray efficiency better than 40%.

Observations are done in an ON/OFF mode: the source is tracked (ON) for ~ 30 minutes and, to estimate the background, the telescope tracks a control region offset in right ascension on the source. Typically, one OFF-region is observed for every two ON-regions. Data are further selected for good sky-conditions and stable detector operation.

3 Source Variability and Light Curve

Here, we include data from Spring 1997 to Autumn 1998, representing a total of ~ 100 hours of observation. The data-set has been further restricted to zenith angles $< 45^\circ$, for which the detector calibration studies have been completed. Figure 1 shows the Mrk 501 nightly integral flux levels above 250 GeV.

In 1997, VHE γ -ray emission was very strong and significant variability was observed in the nightly

averages. The highest flare, recorded on April 16th, 1997 reached about 8 times the Crab level. On the other hand in 1998, the integral flux appears to have been fairly constant and low ($\sim \frac{1}{10}$ of Crab nebula rate).

While variability at a nightly scale is directly seen in Figure 1, the search for intra-night variability has been studied in detail in Renault C., Renaud N. and Henri G. (1998). No significant short-term variability was found.

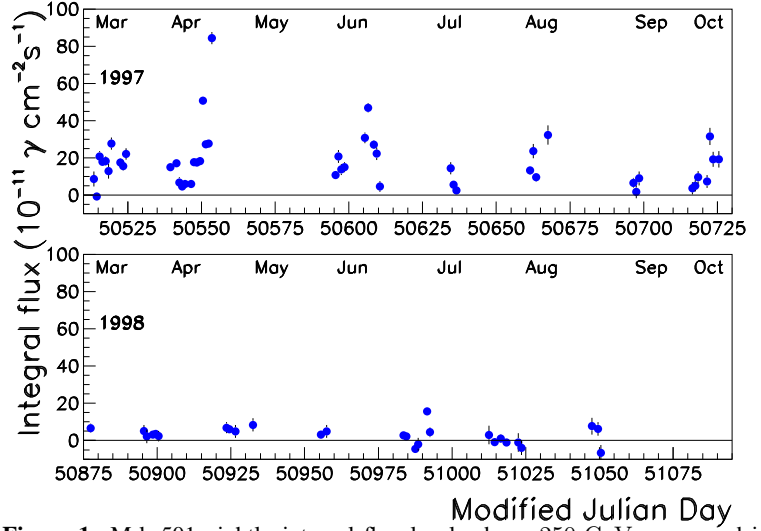


Figure 1: Mrk 501 nightly integral flux levels above 250 GeV, expressed in units of $10^{-11} \text{ cm}^{-2} \text{ s}^{-1}$, for observations in 1997. The average spectral shape as derived in Sect. 4 has been assumed.

4 Differential Energy Spectra

The effective detection area and the energy resolution function are derived from simulations as functions of energy and zenith angle. These simulations take account of the detector response and are calibrated on the basis of the large statistics of gamma-ray excess events from runs on Mrk 501 with a high signal-to-noise ratio, and of Čerenkov rings induced by muons.

The differential energy spectra are obtained, for a given hypothesis on the spectral shape, by a

maximum-likelihood fit taking into account the effective area and the energy-resolution function of the telescope. Two possible spectral shapes have been investigated: a pure power law (\mathcal{H}_0) and a curved shape (\mathcal{H}_1) defined by $\phi_0 E_{\text{TeV}}^{-(\alpha+\beta \log_{10} E_{\text{TeV}})}$, suggested by general considerations on γ -ray emission from blazars. The likelihood ratio of the two hypotheses, defined as $\lambda = -2 \times \log \frac{\mathcal{L}(\mathcal{H}_0)}{\mathcal{L}(\mathcal{H}_1)}$, gives an estimate of the relevance of \mathcal{H}_0 with respect to \mathcal{H}_1 .

For this spectral analysis, the dataset was taken from March to October 1997. During this period, three different activity states of Mrk 501 have been defined: *HF* for high-intensity flares with an integral flux ($\geq 50 \times 10^{-11} \text{ cm}^{-2} \text{ s}^{-1}$), *LF* for low-intensity runs with an integral flux ($\leq 12 \times 10^{-11} \text{ cm}^{-2} \text{ s}^{-1}$) and

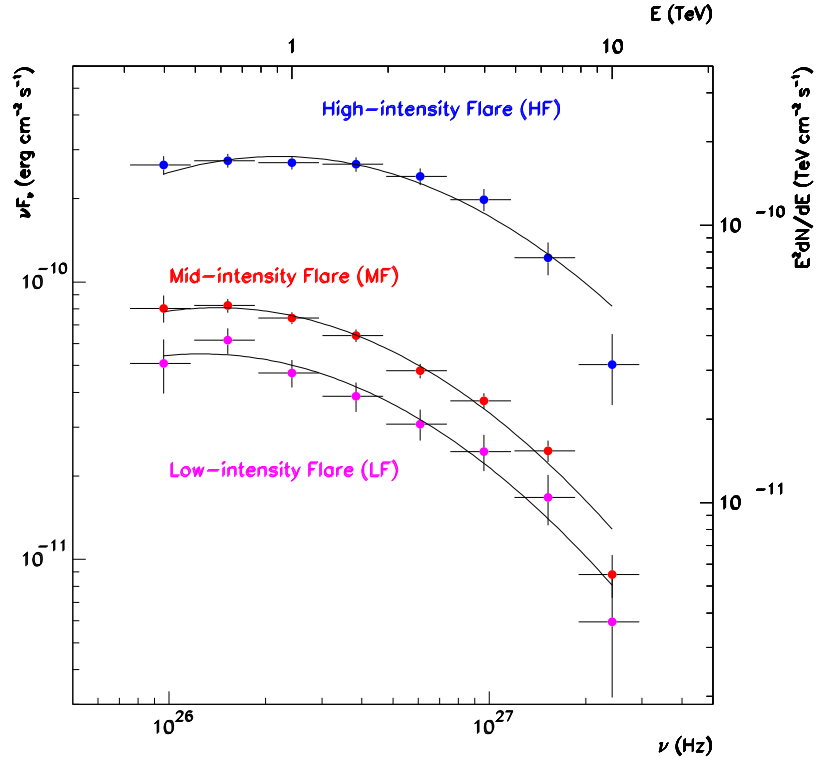


Figure 2: νF_ν or $E^2 d\Phi/dE$ spectra for the HF, MF, and LF states. Individual intensities per bin are only indicative.

MF for mid-intensity flares with an integral flux between *HF* and *LF*. The average over the complete data-set (*AV*) has also been considered. Results for each data-subset are given in Table 1. Only statistical errors are quoted in this table.

The resulting differential energy spectra of Mrk 501 are shown for energies from 330 GeV up to 10 TeV in Figure 2. The likelihood ratio, λ , behaves like a χ^2 with one degree of freedom. Thus, from the values of λ , the probabilities of falsely accepting \mathcal{H}_1 , over \mathcal{H}_0 , are 7×10^{-8} and 7×10^{-12} respectively, if the power-law hypothesis were true. The weak intensity of the source in the LF state may explain the lower significance of the curvature term β in this state. The VHE peak emission of Mrk 501 clearly takes place in the range of several hundred GeV. The corresponding peak energies, E_{\max} , in the spectral energy distribution ($E^2 d\phi/dE$) have been derived from the fitted values of α and β (Table 1).

There is some indication of an increase in E_{\max} with source intensity, which is equivalently shown by the variation of the fitted values of α , corresponding to a possible correlation between intensity and E_{\max} . The intensity-hardness correlations, discussed in the next section, support this effect. Moreover, a correlated variability in X-ray and γ -ray have been observed (Djannati-Atai et al., 1999). So, together with the power deficit in the GeV range (Samuelson et al., 1998), this strongly suggests a two-component emission spectrum for Mrk 501 (Fossati et al., 1998).

Table 1: The differential flux is given in units of $10^{-11} \text{ cm}^{-2} \text{ s}^{-1} \text{ TeV}^{-1}$. In the hypothesis of a curved shape (\mathcal{H}_1), it is parametrized as $d\phi/dE_{\text{TeV}} = \phi_0 E_{\text{TeV}}^{-(\alpha+\beta \log_{10} E_{\text{TeV}})}$. ϕ_0^{pl} and α^{pl} refer to a pure power-law hypothesis (\mathcal{H}_0). The fit has been performed in the interval from 330 GeV-13 TeV. The last columns give the peak-emission energies E_{\max} .

Set	ON (h)	ϕ_0^{pl}	α^{pl}	ϕ_0	α	β	λ	E_{\max} (GeV)
LF	13.6	2.72 ± 0.13	2.45 ± 0.05	3.13 ± 0.19	2.32 ± 0.09	0.41 ± 0.17	10.7	410 ± 201
MF	40.5	4.10 ± 0.10	2.46 ± 0.03	4.72 ± 0.14	2.25 ± 0.05	0.52 ± 0.08	47.1	583 ± 104
HF	3.1	14.5 ± 0.50	2.21 ± 0.03	17.6 ± 0.61	2.07 ± 0.04	0.45 ± 0.09	29.1	840 ± 108
AV	57.2	4.56 ± 0.10	2.46 ± 0.02	5.19 ± 0.13	2.24 ± 0.04	0.50 ± 0.07	61.5	578 ± 98

5 Source Intensity vs. Spectral Hardness

The hardness ratio is defined as $R = \frac{N_{E>E_{\text{mid}}}}{N_{E>E_{\text{low}}}}$, where $N_{E>E_{\text{low}}}$ (resp. $N_{E>E_{\text{mid}}}$) is the number of events with a fitted energy greater than E_{low} (resp. E_{mid}).

All data have been divided into five sets with different average fluxes. For each data-set the hardness ratio has been computed for three different energy bands, $[E_{\text{low}}, E_{\text{mid}}]_{\text{GeV}} = \{[450, 900]; [600, 1200]; [900, 1500]\}$, hereafter referred to as $R_{[>900/>450]}$, $R_{[>1200/>600]}$, and $R_{[>1500/>900]}$. This method is more robust than the usual spectrum analysis for the following reasons:

- since data have been divided into two bins in energy, statistical fluctuations on the single parameter R are reduced;
- E_{low} is always chosen well-above the detector threshold in order to have a good estimation of the energy;
- the data set is limited to zenith angles $< 25^\circ$ in order to avoid large threshold variations;
- finally, an additional cut on the shower impact parameter (required to be $< 130\text{m}$) allows the energy resolu-

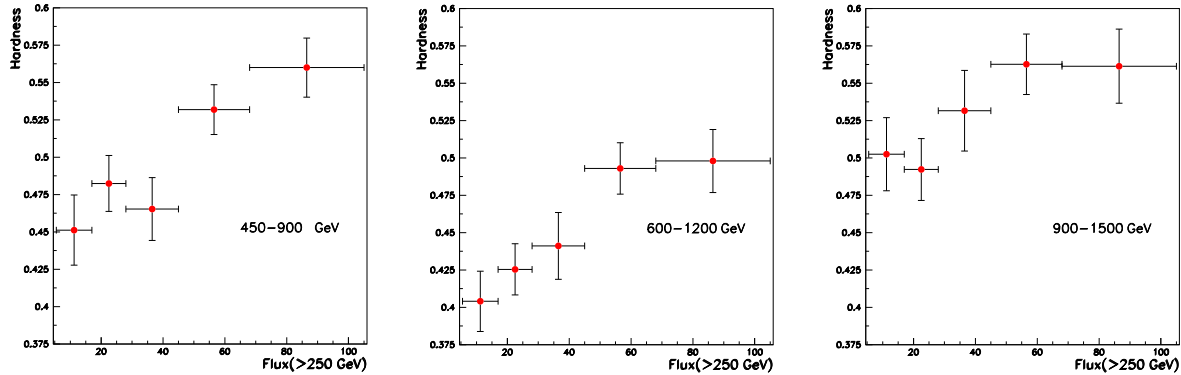


Figure 3: Hardness-ratio vs. source intensity for three different energy bands. Intensities are given as the integral flux above 250 GeV in units of $10^{-11} \text{ cm}^{-2} \text{ s}^{-1}$.

tion to be improved.

The hardness ratio for the three different energy bands is shown in Figure 3. A correlation between hardness and intensity is clearly observed for all energy-bands. The χ^2 probabilities that the distributions are flat for $R_{[>900/>450]}$, $R_{[>1200/>600]}$ and $R_{[>1500/>900]}$ are: 3.8×10^{-4} , 9.0×10^{-4} , and 7×10^{-2} , respectively.

6 Conclusions

The emission from Mrk 501 in 1997 and 1998 has been monitored with the CAT telescope. The spectrum has been measured from 330 GeV up to 10 TeV in 1997, revealing several spectral properties. A curved spectral shape has been derived, confirming the curvature reported by the Whipple group (Samuelson et al., 1998) and HEGRA collaboration (Aharonian et al., 1999). The emission is seen to extend above 10 TeV. The observed intensity-hardness correlation can be simply ascribed to a shift of the peak TeV emission energy. This is confirmed by the observed increase in E_{max} derived from the spectral analysis.

References

- Aharonian et al. 1999, to be published in A&A.
- Barrau, A., et al. 1998, Nucl. Instr. Meth. A416, 278
- Bradbury, S., et al., 1997, A&A 320, L5
- Djannati-Atai, A. et al., 1999, submitted to A&A
- Fossati G., Maraschi, L., Celotti, A., Comastri, A. and Ghisellini, G., 1998, MNRAS, 299, 433
- Le Bohec, S., et al. 1998, Nucl. Instr. Meth. A416, 425
- Protheroe, R.J., et al., 1997, Proc. 25th ICRC (Durban), vol. 8, p. 317
- Punch, M. 1997, Proc. 25th ICRC (Durban), vol. 3, p. 253
- Quinn, J., et al., 1996, ApJ, 456, L83
- Renault C., Renaud N. and Henri G. 1998, the 19th Texas Symposium on Relativistic Astrophysics and Cosmology, held in Paris, France, Dec. 14-18, 1998. Eds.: J. Paul, T. Montmerle, and E. Aubourg (CEA Saclay)
- Samuelson, F., et al., 1998, ApJ, 501, 17